Proceedings of GT2005
ASME Turbo Expo 2005: Power for Land, Sea and Air
June 6-9, 2005, Reno-Tahoe, Nevada, USA

GT2005-68829

DETAILED CHEMICAL KINETIC MODELING OF JP-8/JET-A IGNITION AND COMBUSTION

M. A. Mawid & T. W. Park

Engineering Research and Analysis Company

B. Sekar & C. Arana

Turbine Engine Division
Air Force Research Laboratory
Wright-Patterson AFB, OH 45433

ABSTRACT

Significant progress towards development and validation of a detailed chemical kinetic mechanism for the US Air Force JP-8 fuel is presented in this article. Three detailed chemical kinetic mechanisms for three JP-8 surrogate fuels, as given in Table I, were developed and reported in this study. The main objective is to investigate the performance of the developed three mechanisms for three different surrogate fuel blends and determine the suitability of each mechanism to chemically model the US Air Force petroleum-derived JP-fuel. The detailed JP-8 chemical kinetic reaction mechanism, we have been developing [1-3] for a 12-component surrogate fuel blend, has been used as a basis for the development of two additional detailed reaction mechanisms for the other two surrogate fuel mixtures. Submechanisms for the monosubstituted aromatics such as toluene, m-xylene, butylbenzene, and for the bicyclic aromatics such as 1-methylnaphthalene were all assembled and integrated with the detailed JP-8 reaction mechanism [1-3]. Pressure-dependent rate parameters up to 10 atmospheres for 41 reactions were also included. The three mechanisms were evaluated by predicting the ignition and combustion characteristics of a JP-8 fuel-air mixture in Plug Flow Reactor (PFR) and a Perfectly-Stirred Reactor (PSR) over a temperature range of 933-1020 K and pressure of 1 atm. The results indicated that overall the mechanism for the 6-component JP-8 surrogate 3 (Table I) can predict similar ignition-delay periods as those predicted by the 12-component JP-8 surrogate fuel 1 for atmospheric pressure condition. However, the PSR calculations pointed out to the existence of differences in lighter hydrocarbon species concentration profiles such as CH4, C2H4, C3H6, and C4H8 and important emission species such as CO and CO2 as predicted by the mechanisms that exhibited comparable ignition delay times. The study suggests that, for the conditions considered here, that the developed mechanisms still require further evaluation under various combustion environments, including transport phenomena, to determine the suitability of the chemical kinetic mechanism for either surrogate fuel 1 or 3 to chemically simulate the actual US Air Force JP-8 fuel.

INTRODUCTION

To achieve significant reduction in the development cost and time of military gas turbine combustors, whether they are new or derivatives/growth of existing combustors, substantial reliance upon computer-based CFD simulations and combustion models to predict combustor performance would be required. The quality of the predicted combustion processes such as ignition delay times, flame speed, flame blowout, pollutant emissions, and combustion efficiency is strongly dependent on the oxidation mechanism used to model the wide variety of fuel components present in practical aviation fuels such as JP-8/Jet-A and their interactions in fuel blends. Chemical kinetic reaction mechanisms that describe fuel oxidation processes are essential components in the modeling of the interactions between fluid mechanics and chemistry. Detailed reaction mechanisms have been developed for smaller alkanes [4-6], alkenes such as

ethylene [7-11] and 1,3-butadiene [12]. Progress has also been made for more complex hydrocarbons such as benzene [13], toluene [14], n-heptane [15,16] and n-decane [17,18]. Such detailed mechanisms contain large numbers of chemical species and elementary chemical reactions and can not readily be applied to the modeling of multi-dimensional fluid flow problems. Furthermore, current Computational Fluid Dynamics (CFD) techniques that attempt to combine such detailed reaction mechanisms with accurate closures for other processes, notably turbulence-chemistry interactions, encounter prohibitive computational difficulties primarily due to the substantially increased computational times. Recent work on turbulent reacting flows using transported PDF methods [19] has shown that modeling of kinetically influenced phenomena, such as pollutant emissions and extinction/re-ignition cycles requires accurate chemical descriptions. The problem can be made manageable by using very simplified reaction or global mechanisms, that give an overall description of the reaction process. However, while some overall flame properties can be captured by global mechanisms the overall accuracy is typically insufficient to model key practical phenomena such as flame stabilization in high performance military propulsion devices. Chemical kinetic data that describe the combustion phenomena accurately and serve as a starting point for the development of simplified reaction schemes suitable for three-dimensional calculations of turbulent flows are still needed.

The situation with respect to practical aviation fuel blends is still more complex due to the multitude of fuel components. Progress towards the development of detailed reaction mechanisms for fuels such as JP-8/Jet-A and kerosene has been made [1-3,17-18,20-23]. In several of these studies the assumption of abstraction followed by thermal decomposition of the primary radical has been used as a preliminary basis. The classical abstraction/alkyl radical decomposition concept [24] has thus been used to construct kinetic mechanisms for fuels such as octanes [25], JP-8 [1-3,23], and JP-7 [2-3]. A particular difficulty identified is that the decomposition products of many of the alkyl radicals remain unknown along with their kinetic rate parameters.

A key issue in the development of suitable detailed reaction mechanisms rests with the intended domain of applicability. The complexity necessary to describe phenomena such as (auto-) ignition, ignition delay and pollutant emissions pertinent to signature issues varies significantly. Further challenges arise in the development of an oxidation mechanism for JP-8/Jet-A fuels due to the fact that these petroleum-derived fuels contain as many as 1000 compounds [26]. In addition, the chemical composition may vary depending upon the source of the petroleum fuel. Therefore, in order to study these petroleum fuels and develop adequate detailed kinetics mechanisms, consistency needs to be maintained. One method of assuring the latter for the purpose of kinetic development, is to establish surrogate fuels that have similar physical and chemical properties to practical, petroleum-derived fuels. Such "model" fuels can be composed of a relatively small number of pure hydrocarbons available commercially. Schulz [26] formulated a surrogate blend of 12 pure hydrocarbons (Table I) (iso-octane, cyclooctane, decane, dodecane, tetradecane, hexadecane, methyl-cyclohexane, m-xylene, 1,2,4,5-tetramethyl-benzene, butyl-benzene, tetralin and 1-methyl-napthalene) to simulate the distillation and compositional characteristics of a practical JP-8 fuel. Violi et al. [27] also developed two surrogate fuel blends using 6 pure hydrocarbons (Table I) to represent JP-8 fuels which have less aromatic components than that developed by Schulz [26]. The compounds used in the three surrogate fuels above fall essentially under four classes: alkanes, cyclo-alkanes, single ring aromatics and multiple ring aromatics. The chemical complexities increase significantly with each class and the oxidation of multiple ring aromatics poses significant fundamental challenges. Accordingly, past efforts have typically been aimed at reducing the number of surrogate fuel components to a minimum or by the introduction of global simplifications. Gueret et al. [28] modeled kerosene oxidation via quasi-global models for n-decane, n-propyl-cyclohexane, trimethyl-benzene, xylene, toluene and benzene, and the need for further refinements in the aromatic models was recognized. Dagaut et al. [29] modeled kerosene using n-decane as a surrogate fuel and neglected aromatic components. Vovelle et al. [30] modeled the aromatic component using a simplified toluene mechanism. Lindstedt & Maurice [18] modeled kerosene oxidation using detailed reaction mechanisms for n-decane, toluene, benzene and ethyl-benzene. Mawid et al. [1-3,23] modeled JP-8 combustion through the application of simplifying assumptions for the fuel components suggested by Schulz [26] and Violi et al. [27].

The surrogate fuel blends may naturally be constructed with various volume percents for the various components considered and the choices made validated against experimental data for properties such as the distillation characteristics of the fuel. Both Violi et al. [27] and Schulz [26] selected the pure hydrocarbons in such a way as to reproduce the boiling point curve of the petroleum-derived Wright-Patterson Air Force Base (WPAFB) JP-8 as shown in Fig, 1. The boiling point distributions of surrogate JP-8 blends has been shown to reasonably match the actual fuel and Fig.

1 shows an experimental comparison between the JP-8 surrogate blends and the WPAFB JP-8 for component recovery (Recovery Distillation Curve). It can be seen that overall the JP-8 surrogate blends and the actual WPAFB JP-8 have similar distillation curves in 20-90 volume percent boiling off range. In the 0-20 volume percent boiling-off range, JP-8 surrogate blends 2 and 3 (Table I) are seen to have a slightly larger concentration of lighter branched paraffins such as methylcyclohexane. However, towards the higher end, the experimental WPAFB JP-8 and surrogate blend 1 are very close, indicating that the presence of hexadecane in the mixture blend is important in this context.

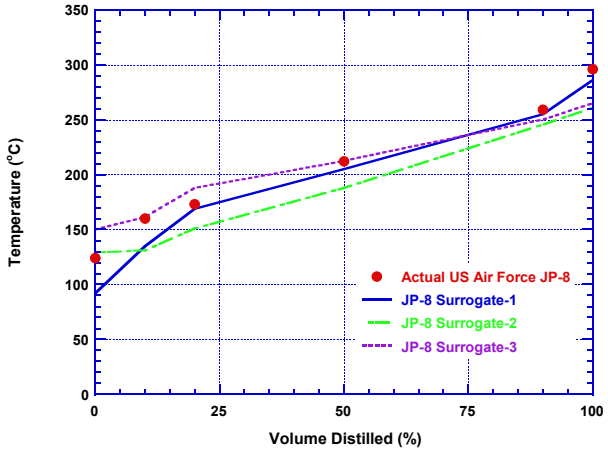

Figure 1. Boiling-Point Recovery Curves for the Actual USAF JP-8 and the JP-8 Surrogate Blends.

It is perhaps evident from the above discussion that the principal challenge is to retain a balance between mechanism complexity and sufficient accuracy with respect to the selected key parameters of interest. The latter can be ignition and emissions characteristics, high temperature oxidation behavior in a combustor or, as shown above, the boiling point recovery curve. Irrespective of the phenomena of interest, it is evident that any surrogate fuel should contain a mixture of at least one component of each of the above classes and in the context of a JP-8 fuel it is imperative that any attempt must take into account the correct volume percent of the aromatics, olefins, paraffins and monocycloparaffins. In addition, the fuel must contain the correct weight percent of hydrogen.

As indicated above, the primary objective of the present study is to further evaluate the three detailed chemical kinetic mechanisms for the three JP-8 surrogate fuels by modeling ignition and oxidation of a premixed JP-8 fuel-air mixture in flowing (PFR) and PSR systems and comparing the predictions to the available experimental data for Jet-A fuel. In addition, by considering various surrogate fuel mixtures, an assessment of the complexity of the detailed reaction mechanisms may be made. The detailed chemical kinetic reaction mechanism, we have been developing [1-3,23], for the oxidation of the Air Force JP-8 fuel will be used as a basis for the present efforts here and the additional needed submechanisms will be developed and assembled with the parent JP-8 mechanism.

The results demonstrated that for the conditions considered in the present analysis, the auto-ignition delay times as predicted by the 12 and 6-component (surrogate 3, Table I) were in satisfactory agreement with measured data. However, the oxidation of the same JP-8 fuel-air mixture in a PSR showed that the predicted intermediate and final species profiles as a function of the PSR residence time using the mechanisms for surrogate fuels 1 and 3 (Table I) are different. The implication of these findings is that further vigorous detailed chemical kinetics analysis and comparisons with data still needs to be carried out to determine the relative suitability of each mechanism for each JP-8 surrogate fuel composition to chemically simulate the petroleum-derived WPAFB JP-8 fuel.

An overview JP-8 detailed kinetic reaction development approach will be given in the next section followed by results and finally conclusion.

OVERVIEW OF LOW AND HIGH TEMPERATURE HYDROCARBON REACTION OXIDATION

The complexity of the low and high temperature JP-8 oxidation indicates that, a detailed scheme typically involves several hundred chemical species taking part in thousands of elementary reactions. However, only a very limited number of different reaction types usually take place [31]. These types include alkane (RH) thermal decomposition, H-atom abstraction to form an alkyl radical, alkyl radical isomerization and β-decomposition of the alkyl radical for the high temperature range, given as

H-Abstraction Reaction:

$$RH + X \rightarrow R + XH \quad (X = H, O, OH, O2, HO2, CH3) \qquad (1)$$

where R is the alkyl radical

Isomerization Reactions:

$$R \rightarrow R' \qquad (2)$$

β-Decomposition of Alkyl Radicals:

$$R \rightarrow Rs + Olefins \quad (3)$$

Thermal Decomposition of Parent Hydrocarbon RH:

$$RH \rightarrow R1 + R2 \quad (4)$$

where R1 & R2 are about equally heavy smaller radicals

Alkanes are initially attacked by H, O and OH radicals generated in the oxy-hydrogen reaction. The alkyl radicals formed this way decompose to smaller alkyl radicals by fast thermal elimination of alkenes. Only the relatively slow thermal decomposition of the smallest alkyl radials, CH3 and C2H5 compete with recombination and oxidation reactions by O atoms and O2. This part of the mechanism is rate-controlling in the combustion of alkanes and alkenes and must be described by a detailed mechanism consisting of elementary reactions. Alkyl radical decomposition and reactions leading to C1- and C2-fragments are too fast to be rate-limiting and can therefore be described by simplified reaction schemes discarding alkyl isomeric structures.

The first attack on the alkane is provided by H, O, and OH radicals generated in the chain-branching steps of the oxygen-hydrogen reaction system. Attacks by HO2 or alkyl radicals on the alkane are too slow to be important. In general there are four possible types of reaction after the 1st attack by O/H/OH based upon the combustion temperature. These possible types are as follows,

1. Thermal decomposition by elimination of alkene to form smaller alkyl radical
2. Reaction with O2 to form alkene
3. Reaction with O to form an aldehyde and a smaller alkyl radical
4. Recombination and disproportionation with another alkyl radical or H atom

Thermal decomposition is the only relevant reaction of the higher alkyl radicals in high temperature combustion. Only the relatively slow thermal decomposition of the smallest alkyl radicals such as CH3 competes with recombination and oxidation reactions by O atoms and O2. Therefore, this part of the reaction mechanism is rate-controlling in the combustion of alkanes and alkenes. This is the reason why all detailed reaction mechanisms for alkyl radical decomposition are still lacking due to the large number of alkyl isomeric structures and the necessary resulting number of potential reaction paths. For example, the number of C8H17 and C7H15 radicals, after the H, O, and OH attack on octane and heptane, is about 89 and 39, respectively [32].

The low temperature part of the reaction mechanism involves the O2 molecule [31,33], which attacks alkane (RH) to produce the alkyl radical R and HO2. This alkyl radical reacts with O2 to produce an alkylperoxy radical RO2 as

$$R + O2 \leftrightarrow RO2 \quad \text{(first O2 addition)} \quad (5)$$

If the temperature increases, RO2 radical decompose back to the reactants. This leads to an inverse temperature dependence of the reaction [34-35] (i.e., degenerate chain branching). The radical RO2 can then undergo either external or internal H-atom abstraction, for external reactions, which are relatively slow [33,36]:

$$RO2 + RH \rightarrow ROOH + R \quad (6)$$

$$ROOH \rightarrow RO + OH \quad \text{(chain branching)} \quad (7)$$

For internal H-atom abstraction:

$$RO2 \rightarrow QOOH \quad \text{(internal abstraction)} \quad (8)$$

$$QOOH \rightarrow QO + OH \quad \text{(chain propagation)} \quad (9)$$

$$QOOH \rightarrow Q + HO2 \quad \text{(chain propagation)} \quad (10)$$

where QOOH is an alkylhydroperoxy radical with fuel structure, Q is an olefin, and QO is cyclic ether. The second chain branching precursors QOOH can react with O2 and lead to extensive chain branching and accelerated ignition as [37]

$$QOOH + O2 \leftrightarrow O2QOOH \ (2^{nd} \text{ O2 addition}) \quad (11)$$

The O2QOOH radical can then undergo external or internal H-atom abstraction. The external H-atom abstraction reactions are also relatively less important than the internal ones and are given as

$$O2QOOH + RH \rightarrow HO2QOOH + R \quad (12)$$
(external abstraction)

$$HO2QOOH \rightarrow HO2QO + OH \quad (13)$$
(chain branching)

$$HO2QO \rightarrow OQO + OH \quad (14)$$
(chain propagation)

The internal H-atom abstraction reactions are given as

$$O2QOOH \rightarrow HO2Q'OOH \quad (15)$$
(internal abstraction)

$$HO2Q'OOH \rightarrow HO2Q'O + OH \quad (16)$$
(chain branching)

$$HO2Q'O \rightarrow OQ'O + OH \quad (17)$$
(chain branching)

The radicals OQO and OQ′O can then decompose via β-decomposition into two other oxygenated species such as aldehydes. Reactions (16) and (17) are the chain branching reactions responsible for distinct acceleration of the ignition process. This effect and the degenerate branching behavior are responsible for the experimentally observed negative temperature dependence of the ignition delay time at low temperatures.

The OQO and OQ′O can decompose to oxygenated aldehydes RCHO, which is then attacked by OH, H, HO2, CH3O2 at low temperatures as [38-39]

$$RCHO + X \rightarrow RCO + XH \quad (18)$$
(X = OH, H, O2, HO2, CH3O2)

The peracyl radicals RCO formed in the above reaction are attacked by a second O2 addition as

$$RCO + O2 \rightarrow RCOO2H \quad (19)$$

The peracyl radicals can then undergo external H-atom abstraction and produce CO2 by the decomposition reaction

$$RCOO2H \rightarrow R + CO2 + OH \quad (20)$$

As the reaction temperature increases, another reaction path is possible that produces CO and an alkyl radical as

$$RCO \rightarrow R + CO \quad (21)$$

The kinetic data for most of the above reactions were compiled from different sources [15,17,20-21,25,29,31-41].

Due to the presence of dozens of alkyl radicals, it would be a formidable task to attempt to develop very detailed mechanisms to describe the complex chemistry of the system of alkyl compounds. However, due to the fact that alkyl radical decomposition and the reaction leading to C1- and C2-fragments are too fast to be rate-limiting, simplified decomposition paths for the large alkyl radicals may be derived. These simplified decomposition paths entail the assumption that the large alkyl radicals isomeric structures are unimportant.

JP-8 FUEL DETAILED CHEMISTRY MECHANISMS DEVELOPMENT

Some reactions from submechanisms such as C1-C6, C7, and C10 developed by Dagaut et al. [17,29], Doute et al. [20], Cathounet et al. [21], Warnatz [40], Axelsson et al. [25], Warnatz et al. [34], Westbrook et al. [32], and Chevalier et al. [33] were used to develop a detailed kinetic mechanism. Submechanisms for the normal paraffins in the surrogate models such as decane, dodecane, tetradecane, and hexadecane were developed and added to the above mechanisms. For isooctane, the mechanism developed by Axelsson et al. [25] was partially used for the development of the detailed JP-8. Submechanisms for the aromatic compounds were also assembled and added to the above submechanisms [42]. The submechanism for dodecane under high and low temperature conditions are given in the next section as an example. Note here that the high and low temperature submechanisms given here were truncated at C7 and C5, respectfully. The additional submechanisms for C1-C7 are not included here due to their significantly larger size.

High Temperature Submechanisms

For high temperature combustion, it is known that the alkyl radical, formed in the initial reaction is decomposed to smaller alkyl radicals by elimination of alkenes as described above. A radical decomposes when a bond is broken. When there is a choice between C-H and C-C bonds, the C-C bond is usually broken due to the lower bond strength. However, as mentioned above, due to the large number of alkyl and alkene isomeric structures, only representative reactions and species are considered along with representative reaction paths. Table II, for example, contains the details of the submechanism only for the primary C-H bonds of n-C12H26. This submechanism for the consumption of n-C12H26 was carried out upon the assumption that under short residence time and high temperature conditions, distinction between various large alkyl radicals was not important. In this submechanism hydrogen abstract was assumed to occur on a secondary carbon atom and only one decomposition path was considered for the radicals C12H25. Similar assumptions were used by Nehse and

Warnatz [31] to model heptane combustion. The submechanism for C6H12 developed by Chakir et al. [15] was used for the remaining reactions of n-C12H26 submechanisms. Submechanisms for decane, tetradecane, hexadecane, MCH, iso-octane, cyclooctane, and aromatic components were developed in a similar manner.

Low Temperature Submechanisms

The low temperature oxidation of JP-8 was developed using the above first and second O2 addition reactions, chain-branching, chain propagation and decomposition. The developed low temperature submechanism for dodecane, for example, is given in Table III. The low temperature submechanism, however, still requires further improvement for determining the kinetic rate parameters and reactions decomposition products, in particular for the 1^{st}-O2 addition reactions.

Benzene, Toluene and M-xylene Submechansims

Additional reactions for benzene and toluene were included into the detailed mechanism to represent the aromatic components of JP-8 in surrogate fuel blends. Benzene is formed primarily by the reactions

$$C3H3 + C3H3 = C6H6 \quad (22)$$

$$C6H5 + H = C6H6 \quad (23)$$

$$C6H5OH + H = C6H6 + OH \quad (24)$$

and

$$C4H5 + C2H2 = C6H6 + H \quad (25)$$

However, if toluene is present in the initial fuel composition, additional benzene is formed through an H-abstraction reaction of the toluene C7H8 as

$$C7H8 + H = C6H6 + CH3 \quad (26)$$

$$C6H6CO + H = C6H6 + HCO \quad (27)$$

and toluene C7H8 can be formed through

$$C4H5 + C3H4 = C7H8 + H \quad (28)$$

Additional benzene was assumed to be produced by the thermal decomposition of m-xylene through the reaction

$$C8H10 \rightarrow C6H6 + C2H4 \quad (29)$$

Linstedt et al. [43] considered additional formation of benzene through the formation of fulvene. The route to fulvene through the methyl-cyclopentadienyl radical as

$$CH3 + C5H5 = C5H4CH3 + H \quad (30)$$

$$C5H4CH3 = C6H6(F) + H \quad (31)$$

$$C6H6(F) = C6H6 \quad (32)$$

was found to be important and contributed 25% of fulvene formation in cyclo-pentene and methyl-cyclopentadiene pyrolysis in a shock tube. These reaction channels were included in the current submechanism for benzene. The destruction submechanism for benzene has been based on the mechanism of Tang et al. [44], Ventkat et al [45], and Lindstedt & Skevis [13] and the mechanisms of Emdee et al. [46] and Lindstedt & Maurice [14] for the oxidation of toluene. The mechanism of Tang et al. [44] has been validated in jet-stirred reactors up to 10 atm. The need to include these submechanisms into the JP-8 detailed mechanism is dictated by the presence of the aromatic components in the petroleum derived JP-8 fuels. The submechanism for the oxidation of m-xylene has been previously developed [1] based upon the four important reaction paths mentioned above. The chemical kinetic rate parameters have been either taken or estimated from existing data in the literature [21,28,47]. Table IV contains the above submechanisms used in the current study.

Thermodynamic Data and Chemical Rate Parameters

Many of the rate parameters in the low and high temperature chemistry of JP-8 surrogate components are unknown or uncertain. Therefore, rate parameters not found in the literature were estimated by analogy with similar reactions. Most of the rate parameters were taken from refs. [13-15,17,20-21,25,29,31-41,44-46]. Reverse rate parameters were computed from the forward rate parameters and appropriate equilibrium constants. These equilibrium constants were calculated using coefficients from CHEMKIN-III database [48]. The unknown thermodynamic data of species appearing in the present mechanism were estimated by using Benson's additivity rule and data [49]. The known thermodynamic data were taken from Burcat's compilation [50].

RESULTS AND DISCUSSION

The current high temperature detailed mechanism consists of 231 chemical species and 1547 chemical reactions developed for the 12-component JP-8 surrogate fuel blend (i.e., surrogate fuel 1 in Table I). As the number of compounds in the surrogate fuel decreases, the number of reactions and species would decrease as well. In the present study, the detailed mechanism for the 12-component JP-8 surrogate was also utilized to model surrogates 2 and 3 as given in Table I after adding a toluene submechanism given in Table IV. In addition, as the range of operating pressure, temperature and stoichiometric conditions, becomes wider, the reaction rates for some reactions will be pressure-dependent. Pressure-dependent reaction rate constants up to 10 atm [17-18,29] for 41 reactions were also assembled and added to the detailed JP-8 mechanism for high pressure combustion conditions. As indicated in previous studies, the long-term conditions of interest for JP-8 mechanism validation are pressures from 1-75 atm, inlet temperatures from 600-1800 K and equivalence ratios in the range 0.3–2.0.

Experimental data on JP-8 ignition/combustion for mechanism validation is almost nonexistent in the open literature for the intermediate and high temperature ranges. For this reason, the developed detailed JP-8 mechanism predictions have so far been compared against auto-ignition delay measurements for Jet-A fuel/air mixture for an equivalence ratio, Φ, of 0.5 (fuel-lean mixture), temperature range of 900-1020 K and initial pressure of 1 atm in a coflowing combustion rig [51-52]. The plug flow equations [53] were used to model fuel-air coflow system [51-52]. The numerical solution of the plug flow equations with chemical reactions was based on CHEMKIN software package [53]. In addition, the perfectly-stirred reactor (PSR) [54] governing equations were employed to model the oxidation of a premixed JP-8-air mixture under the same experiment conditions of Freeman and Lefebvre [51]. Once again, the numerical solution of PSR equations with the detailed JP-8 mechanism was based on CHEMKIN Package.

Ignition Delay Time Calculations

The three JP-8 surrogate fuel blends (i.e., Table I) were evaluated for a lean mixture covering a temperature range of 900-1020 K (representative of intermediate-temperature chemistry) and ambient pressure condition by comparing the computed auto-ignition delay times with the measured data of Freeman and Lefebvre [51], Mullins [52] for Jet-A fuel. Figures 2 and 3 show the temperature-time history of the premixed JP-8/air mixture as it travels in the plug flow reactor and for inlet temperatures of 933 and 1020 K and for the three JP-8 surrogate fuel blends (i.e., Table I). It is seen that after the induction period, ignition takes place, which is manifested in a sharp increase in the temperature. The induction period is predicted to vary with the surrogate fuel blend. For an inlet temperature of 933 K, surrogate fuel blend 2 has the shortest induction period. This surrogate fuel blend 2 behaves in a similar manner for inlet temperature of 1020 K as depicted in Fig. 3. This surrogate fuel blend 2 will, therefore, have the shortest ignition delay time. Surrogate fuel blend 3 is seen to have the same ignition delay times for the two inlet temperatures as those of the 12-component JP-8 surrogate fuel 1. In addition, surrogate fuel blends 2 and 3 predict a higher combustion temperature after ignition occurs than surrogate fuel 1.

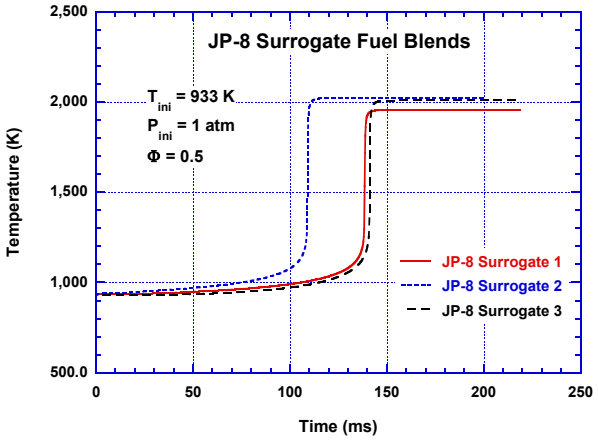

Figure 2. Temperature-Time History of the Premixed JP-8/Air Mixture for Inlet Temperature of 933 K and for the Three JP-8 Surrogate Fuel Blends.

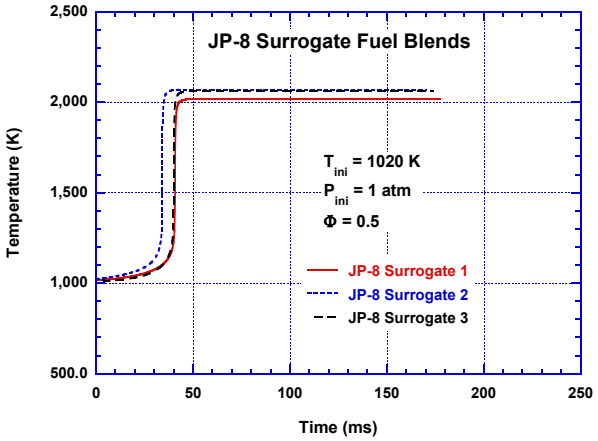

Figure 3. Temperature-Time History of the Premixed JP-8/Air Mixture for Inlet Temperature of 1020 K and for the Three JP-8 Surrogate Fuel Blends.

Figures 2 and 3 clearly demonstrate that the difference in the absolute ignition delay times of the three JP-8 surrogate blends is diminished as the initial mixture temperature is increased. The absolute ignition delay times difference between surrogate fuel blends 3 and 2 is roughly about 32 ms for an inlet temperature of 933 K. Whereas for an inlet temperature of 1020 K, the ignition delay time difference is less than about 10 ms. Note here that the relative difference in ignition delay times remains the same as the initial mixture temperature is increased. The implication of these findings is that as the initial mixture temperature is raised, the significance of the surrogate composition and number of compound classes upon ignition delay times is reduced and ignition is primarily influenced by normal alkanes, cycloalkane and iso-alkanes. A similar behavior was also predicted previously [2-3] by changing the aromatic components types and was attributed to the roles of normal, cyclo, and iso-alkanes in controlling the initial radical pool buildup, which leads to ignition. However, more vigorous analysis is still needed to further support the above findings, in particular for lower initial mixture temperatures.

Figures 2 and 3 also illustrate that surrogate fuel blends 1 and 3 have the same ignition behavior and delay times for almost all the inlet temperatures considered in the study. This implies that surrogate fuel blend 3, which contains half the number chemical components as that of surrogate fuel blend 1, might be adequate to simulate the ignition characteristics of WPAFB petroleum-derived real JP-8 fuel. The finding, however, must be taken with caution due to the limited range of pressure, temperature, and stoichiometry conditions utilized in the present study. Extending the analysis to other operating conditions of interest would, however, require benchmark experiments for predictions validation, which are presently lacking.

Figures 4 and 5 demonstrate the predicted OH radical mole fraction profiles versus time for the three surrogate fuel blends 1, 2, and 3. The instants at which OH peaks for the three surrogate fuel blends are consistent with those of Figs. 2 and 3 for the temperature time history. However, after ignition occurs, the steady-state concentration for surrogate fuel blend 1 is predicted to be lower than that for surrogate fuels 2 and 3. This is caused by the difference in flame temperatures predicted for each surrogate mixture as reflected in Figs. 2 and 3. It is important to note here that the final flame temperature attained by each surrogate fuel is controlled by the composition-weighted mixture specific heat at constant pressure (Cp). Surrogate fuels 2 and 3 have a higher mixture Cp than surrogate fuel 1. For this reason, the predicted steady-state flame temperature and OH concentration are lower than the corresponding ones for surrogate fuels 2 and 3.

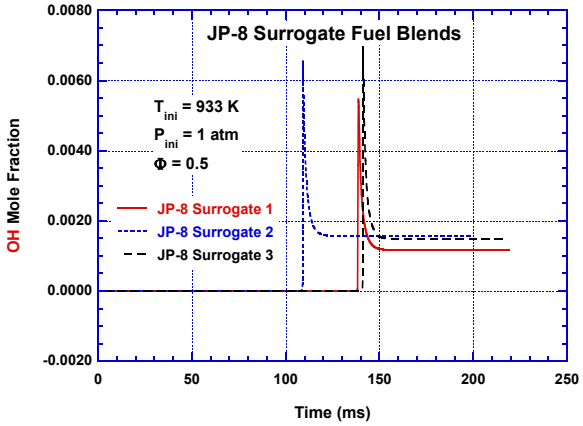

Figure 4. OH Mole Fraction Profiles for Inlet Temperature of 933 K and for the Three JP-8 Surrogate Fuel Blends.

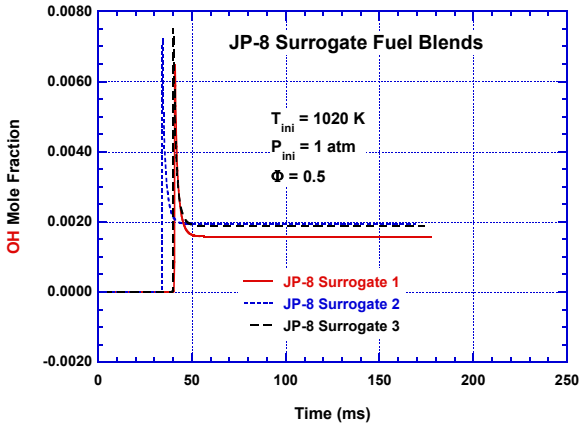

Figure 5. OH Mole Fraction Profiles for Inlet Temperature of 1020 K and for the Five JP-8 Surrogate Fuel Blends.

Figure 6 shows the predicted and measured Jet-A ignition delay times of Freeman and Lefebvre versus the reciprocal of the inlet mixture temperature for the three surrogate fuel blends. Ignition was computed using OH profiles, the time at which OH peaks, which were more accurate than the temperature profiles turning points. The predicted ignition delay times are seen to be influenced by the surrogate fuel blend composition. While surrogate fuels 1 and 3 are observed to have similar ignition delay times, surrogate fuel 2 has shorter ignition delay times than surrogate fuels 1 and 3 over the entire range of inlet temperatures considered. In fact, these predictions lend support to the argument [26-27] that matching the boiling off distribution of WPAFB JP-8 by the surrogate fuel is essential for the development of a reliable "fuel model"

for which a detailed chemical kinetic reaction mechanism may be developed. Violi et al. [27] clearly showed that the volume distillation curve for surrogate fuel 3 in the present study is in better agreement with WPAFB JP-8 distillation curves than surrogate fuel blend 2. It should be noticed here that surrogate fuel blend 1 [26] boiling-off curve has the best agreement with the real WPAFB JP-8 fuel boiling off curve. Overall, it can be stated that for the conditions considered in the present study, the 6-component JP-8 fuel blend 3 [27] is seen to be adequate to simulate and represent the ignition behavior of WPAFB JP-8 as does surrogate fuel blend 1 [26].

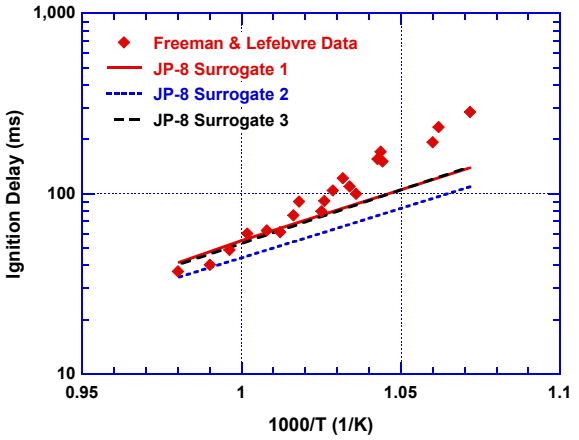

Figure 6. Predicted and Measured Jet-A Ignition Delay Times of Freeman and Lefebvre versus the Reciprocal of the Inlet Mixture Temperature for the Three Surrogate Fuel Blends.

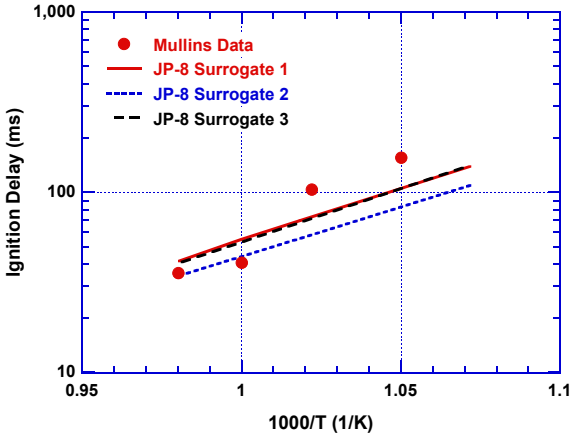

Figure 7. Predicted and Measured Jet-A Ignition Delay Times of Mullins versus the Reciprocal of the Inlet Mixture Temperature for the Three Surrogate Fuel Blends.

To further assess the three surrogate fuel blends ignition delay times, the predicted ignition delays are compared to the ignition data of Mullins as shown in Fig. 7. It is seen that surrogate fuel blends 1 and 3 still exhibit better agreements with the data as compared to surrogate fuel blend 2. It is interesting to note here that the predicted ignition delay times slopes are about the same for all the fuel blends. The difference in the ignition times for the three fuel blends is seen to be constant as the inlet temperature varies. The implication is that the use of various surrogate fuels compositions in the detailed JP-8 mechanism can result only in quantitative and not qualitative variations.

PSR Calculations

To further evaluate the two detailed reaction mechanisms for surrogate fuels 1 and 3, it is always desirable to separate completely any fluid dynamics modeling from the chemistry modeling. Ideally, mechanisms evaluation for comparisons, therefore, should have truly zero dimensions, i.e., no gradients of temperature, species concentration or velocity whatsoever. The closest approach to this ideal would be a Perfectly-Stirred Reactor (PSR), which in theory, has zero gradients of temperature and species concentration, and can be considered one-dimensional in throughput velocity. It is desirable to assess the performance of the developed detailed mechanisms for the same operating conditions as those of the ignition PFR calculations, but over a range of residence times in the PSR. The oxidation of JP-8 fuel-air mixture in a Perfectly-Stirred Reactor (PSR) has, therefore, been investigated under the same pressure, temperature, and stochiometry conditions as those for the ignition analysis above. The objective here is to eliminate any fluid dynamics effects upon the performance of the two detailed chemical reaction mechanisms for the JP-8 surrogate fuels 1 and 3 (see Table I) under steady-state combustion conditions. As presented above, the two JP-8 mechanisms for surrogate 1 and 3 predicted comparable ignition delay times and both were reasonably in agreement with the measured ignition data of Freeman et al. [51] and Mullins [52]. It is, therefore, significant that the two detailed kinetic mechanisms be further evaluated under still a non-transporting combustion environment for the purpose of determining which JP-8 surrogate fuel model should be used as the basis for further development of a detailed JP-8 kinetic reaction. This is also important for conducting experimental investigations to obtain the lacking data for vigorous bench marking of the detailed kinetic model against the data. In the present analysis, the PSR volume was that of the PFR used for the ignition analysis above whose length and side (square) were respectively 220 and 6.2 cm. The PSR computations were carried out at two different inlet temperatures of 933 and 1020 K, at five residence times (0.05, 0.1, 0.15, 0.20, and 0.25 S) at

1 atm, for an equivalence ratio of 0.5. The fuel initial mole fraction for each species is given in Table V. Mole fraction profiles as a function of the inlet temperature and reactor residence time were computed for all initial, intermediate and final species. Of particular interest is the lighter hydrocarbon species profiles such CH4, C2H4, C2H6, C3H6, C4H6, C4H8, and i-C4H8, whose oxidation is rate-determining [1] and their presence in the PSR exhaust is indicative of Unburned Hydrocarbon (UHC) emissions.

Figure 8 shows the calculated final temperature in the PSR as a function of the PSR residence time for two inlet temperatures of 933 and 1020 K, and an equivalence ratio of 0.5, at 1 atm using the initial compositions for surrogate fuels 1 and 3 as given in Table V. It is seen that after the initial increase, both mechanisms for surrogate fuels 1 and 3 maintain a leveled-off temperature with increasing the PSR residence time. For each inlet temperature, the difference in the final exit temperature of the PSR is about 37 K. This small difference in the outlet temperature of the PSR appears to be consistent with the final temperatures for the ignition calculations above (see Figs 2 and 3). However, larger differences are seen in the magnitude of the PFR and PSR final temperatures. For an inlet temperature of 933 K and for surrogate fuel 1, for instance, Fig.2 displays a final temperature of about 1933 K as compared to the PSR final temperature of only about 1753 K. For surrogate fuel 3, the difference in the final temperature of the PFR and PSR is even greater as seen in Figs. 2 and 8. This is indicative of the existence of different initial reactivity in the two chemical kinetic schemes due to different initial compositions for surrogate fuels 1 and 3 and the impact of specific heats at constant pressure (Cp) of the various components upon the final temperature.

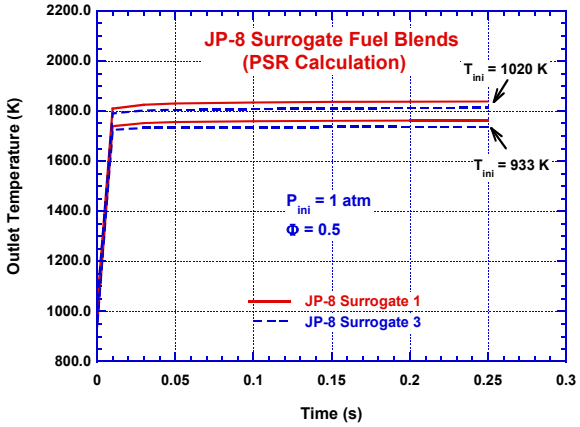

Figure 8. Exit Temperature in the PSR as a Function of the PSR Residence Time.

Figures 9 through 15 illustrate the computed mole fraction profiles plotted against the PSR residence time for CH4, C2H4, C2H6, C3H6, C4H6, C4H8, and i-C4H8 for inlet temperatures of 933 and 1020 K, using JP-8 surrogate fuels 1 and 3 compositions as given in Table V. It is clearly seen that the rates of consumption and/or formation of most of the species as the PSR residence time is increased depend upon the surrogate fuel initial composition. Overall, the detailed chemical kinetic mechanism for surrogate fuel 1 predicts a higher level of species depletion than that mechanism for surrogate fuel blend 3. This appears to be true for both inlet temperatures of 933 and 1020 K with the exception for species C4H6 in Fig. 13. The detailed chemical reaction mechanism for surrogate fuel 1 exhibits a lower level of depletion of C4H6 than the mechanism for surrogate fuel 3. The formation of C4H6 is due to the abstraction reactions acting on the radical C4H7, which is also formed by abstracting one hydrogen atom from butene C4H8. This butene production was assumed to be a product of the decomposition of C10H14 (Butylbenzene). This component is not present in the composition of surrogate fuel 3 as given in Table I. The increased concentration of C4H8 is responsible for lower rate of depletion of C4H6 for surrogate fuel 1. Note here that C4H8 was also assumed to be a product of other decomposition reactions such as C14H29 (tetradecane), which was assumed to thermally decompose into C10H21 and C4H8.

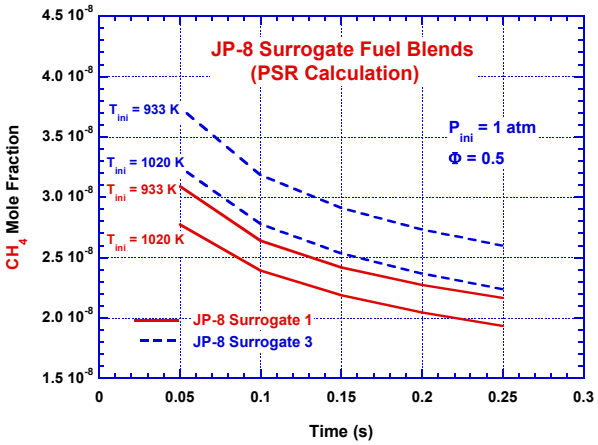

Figure 9. CH4 Mole Fraction Profiles as a Function of the PSR Residence Time.

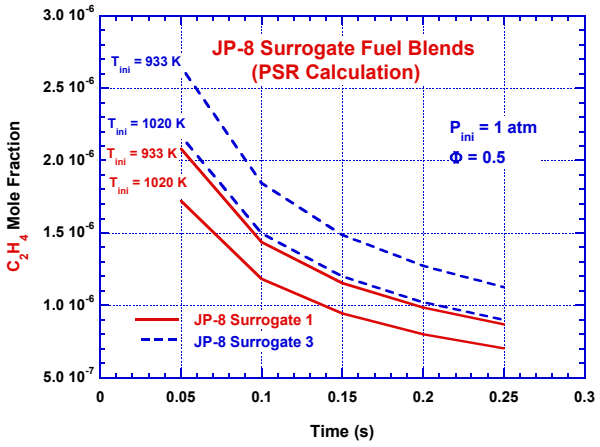

Figure 10. C2H4 Mole Fraction Profiles as a Function of the PSR Residence.

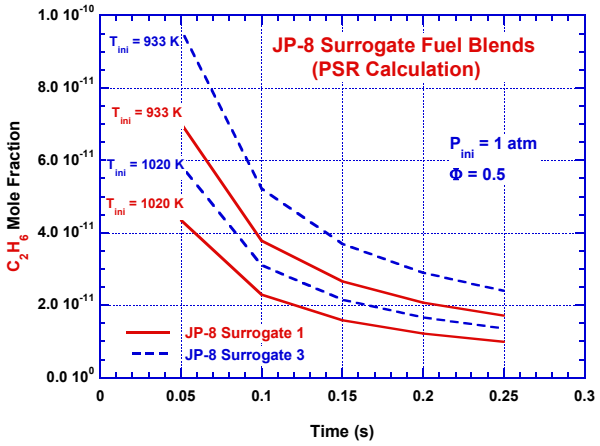

Figure 11. C2H6 Mole Fraction Profiles as a Function of the PSR Residence Time.

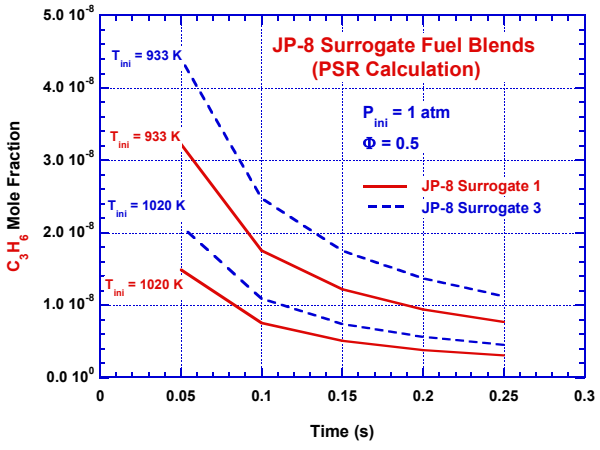

Figure 12. C3H6 Mole Fraction Profiles as a Function of the PSR Residence Time.

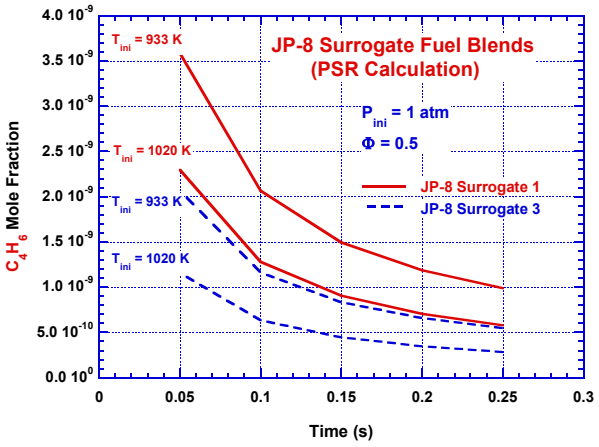

Figure 13. C4H6 Mole Fraction Profiles as a Function of the PSR Residence Time.

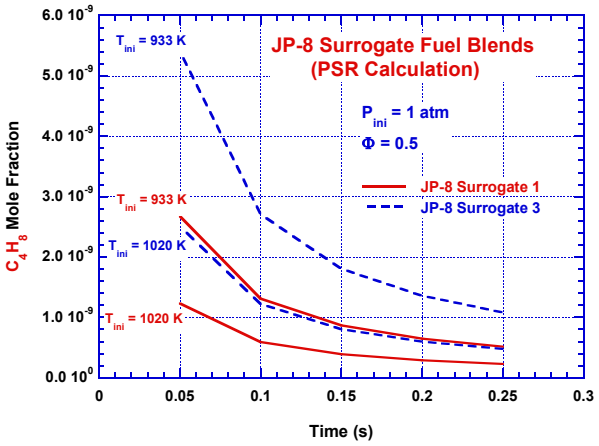

Figure 14. C4H8 Mole Fraction Profiles as a Function of the PSR Residence Time.

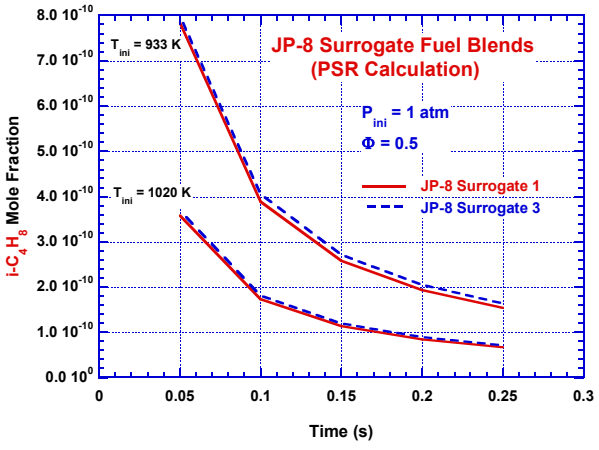

Figure 15. i-C4H8 Mole Fraction Profiles as a Function of the PSR Residence Time.

The predicted profiles for the above species point out to the existence of differences in the species concentration magnitudes at different residence times in the PSR. This implies that certain reactions appear to influence the species profiles more than other reactions for similar reaction channels. Figures 16 and 17 display the temperature sensitivity coefficients for the important reactions for the two mechanisms for surrogate fuels 1 and 3. Note here that the important reactions were defined as the ones having absolute sensitivity coefficients for ignition greater than 0.003. By examining the reaction sensitivity plots, it can be said that the thermal decomposition of normal dodecane NC12H26 into C6H12 and C6H14 is the most important reaction. In addition, the mechanism for surrogate fuel 3, has the last reaction (H+O2+M= HO2+M) as an important reaction with a high sensitivity coefficient. This reaction is not seen to have an important effect on the mechanism for surrogate fuel 1. Note here in the sensitivity plots, the sensitivity coefficient cut off was $1x10^{-4}$. Moreover, the magnitudes of the sensitivity coefficients of the important reactions are observed to be different for the two mechanisms. For example, the third reaction for NC12H26 is the most important reaction for both mechanisms, but it has a higher sensitivity coefficient for surrogate fuel 3 chemical mechanism than the mechanism for surrogate fuel 1. This perhaps explains the qualitative and quantitative similarity in the mechanisms predictions for surrogate fuels 1 and 3 for ignition, and only qualitative similarity in the PSR computations.

It is also of interest to compare the predictions of the two detailed mechanisms for surrogate fuels 1 and 3 for some of the important emissions such as CO, CO2, and H2 in the PSR. Figures 18 through 20 respectively depict the computed CO, CO2, and H2 concentration profiles in PPM versus the residence time for two inlet temperatures of 933 and 1020 K. It is seen that over the entire range of PSR residence times, the detailed mechanism for surrogate fuel 3 predicts lower levels of emissions such as CO and CO2 than the mechanism for surrogate fuel 1. A difference of about 100 PPM for CO for an inlet temperature of 1020 K between the two mechanisms exists. A substantially larger difference in the CO2 emissions predictions can be seen in Fig. 19. These results indicate that the emission levels for UHC in Figs. 9-15, CO, and CO2 as predicted by the two mechanisms for surrogate fuels 1 and 3 are different In addition, the concentration of H2 is also higher for surrogate fuel 1 chemical kinetic mechanism. This further supports the earlier observation that the initial composition of the fuel seems to make a difference in the predicted level of emissions in the PSR. However, as mentioned previously, it is difficult to reconcile the predicted species profiles without having measured species profiles. This once again points out to the urgent need to conduct combustion experiments using the two JP-8 surrogate fuels 1 and 3 to benchmark the developed detailed mechanisms.

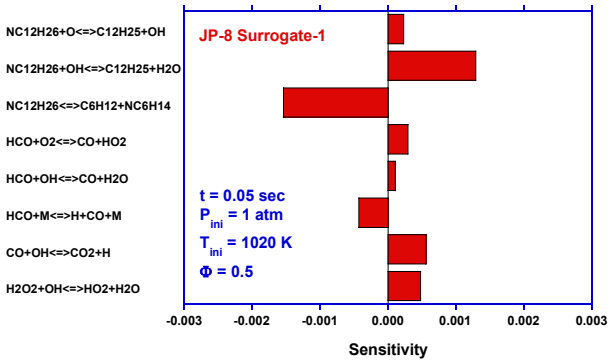

Figure 16. Sensitivity Coefficients for the Important Reactions for Surrogate Fuel 1.

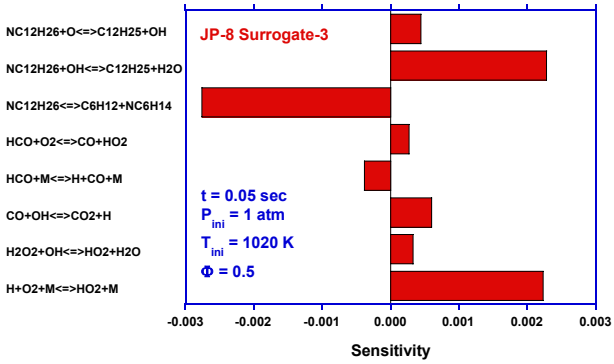

Figure 17. Sensitivity Coefficients for the Important Reactions for Surrogate Fuel 3.

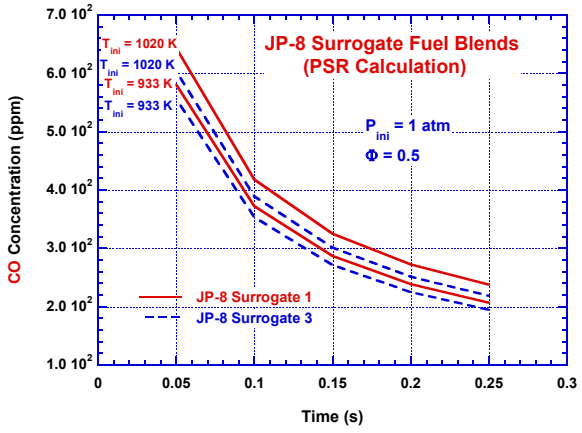

Figure 18. CO Concentration Profiles in PPM as a Function of the PSR Residence Time.

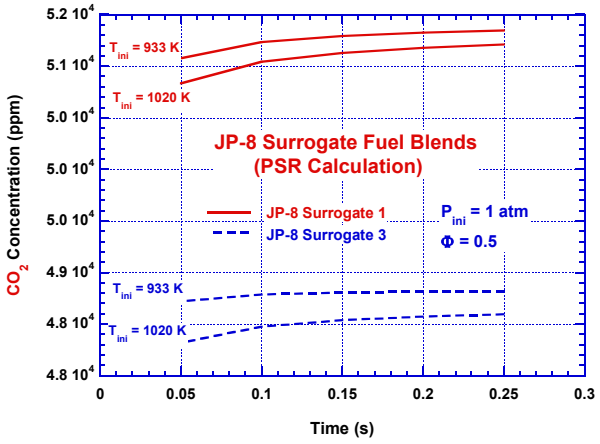

Figure 19. CO2 Concentration Profiles in PPM as a Function of the PSR Residence Time.

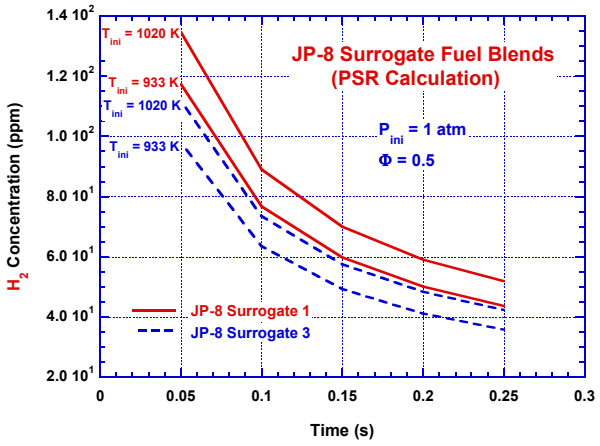

Figure 20. H2 Concentration Profiles in PPM as a Function of the PSR Residence Time.

CONCLUSION

Three detailed chemical kinetic reaction mechanisms were developed to simulate the petroleum-derived WPAF JP-8 fuel. The reaction mechanisms were based upon three different initial chemical compositions representing three JP-8 surrogate fuel blends as given in Table I. Submechanisms for the monosubstituted aromatics such as toluene, m-xylene, butylbenzene, and for the bicyclic aromatics such as 1-methylnaphthalene were assembled and integrated with the detailed JP-8 reaction mechanism [1-3]. In addition, pressure-dependent rate parameters up to 10 atmospheres for 41 reactions were also included in the detailed mechanisms. The performance of the three chemical kinetic mechanisms was investigated in the context of detailed chemical kinetics modeling of auto-ignition delay times of premixed JP-8/air flowing into a Plug Flow Reactor (PFR) and a Perfectly-Stirred Reactor (PSR). Auto-ignition delay times for three JP-8 surrogate fuel blends were predicted and compared with the available ignition delay-times for Jet-A fuel using the three detailed chemical kinetic reaction mechanisms for JP-8. The computed auto-ignition delay times for the three chemical kinetic mechanisms for the three surrogate fuel blends indicated that the mechanism for the 6-component surrogate fuel blend (surrogate 3) with toluene as an aromatic component predicted ignition delay times that are in agreement with the Jet-A data as that mechanism for surrogate fuel blend 1, given in Table I with 12-component in a PFR. However, the two mechanisms for surrogate fuels 1 and 3, which predicted comparable ignition delay times, predicted different rates of consumption/formation of lighter hydrocarbon species such as CH4, C2H6, C3H6, and C2H4 in a PSR under similar conditions as that of the PFR. In addition, the PSR computations revealed differences in the predicted important emission profiles such as CO and CO2 using the detailed mechanisms for surrogate fuels 1 and 3. Therefore, it is concluded that while the mechanism for 6-component surrogate fuel blend 3 [27] is adequate to be utilized to model the actual WPAFB JP-8 fuel ignition under the conditions of the present study, it is unclear at this point that the same mechanism for surrogate fuel 3 can be utilized to predict other combustion phenomena such pollutant missions. It is, therefore, critical that combustion experiments to obtain data for JP-8 fuel under a wide range operating pressure, temperature and stoichiometry conditions be conducted. This warrants additional JP-8 mechanism development and experimental efforts.

REFERENCES

1. Mawid, M. A., Park, T. W., Sekar, B., and Arana, C., "Development and Validation of a Detailed JP-8 Fuel Chemistry Mechanism," AIAA Paper 2002-3876, 38th AIAA Joint Propulsion Conference, Indianapolis, Indiana, July 7-10, 2002.
2. Mawid, M. A., Park, T. W., Sekar, B., and Arana, C., "Development of Detailed Chemical Kinetic Mechanisms for Ignition/Oxidation of JP-8/Jet-A/JP-7 Fuels," ASME Paper 2003-GT-38932, ASME Turbo Expo, Atlanta, Georgia, June 16-19, 2003a.
3. Mawid, M. A., Park, T. W., Sekar, B., and Arana, C., "Development and Validation of Detailed and Reduced Chemical Kinetic Mechanisms for Oxidation of JP-8/Jet-A/JP-7 Fuels," ISABE-2003-1028, XVI ISABE Proceedings, Cleveland, Ohio, August 31 – September 5, 2003b.

4. Westbrook, C. K. and Dryer, F. L.,"Chemical Kinetic Modeling of Hydrocarbon Combustion," Prog. Energy. Combust. Sci., Vol. 10, pp.1-57, 1984.
5. Paczko, G., Lefdal, P.M., and Peters, N., "Reduced Reaction Schemes for Methane, Methanol and Propane Flames," 21st Symposium on Combustion, the Combustion Institute, pp. 739-748, 1986.
6. Leung. K.M. and Lindstedt, R.P. "Detailed Kinetic Modelling of C_1-C_3 Alkane Diffusion Flames", Combustion and Flame 102:129, 1995.
7. Singh, D. J. and Jachimowski, C. J., "Quasiglobal Reaction Model for Ethylene Combustion", AIAA Journal, Vol. 32, No. 1, pp. 213-216, 1994.
8. Dagaut, P., Boetiner, J. C., and Callard, M., "Kinetic Modeling of Ethylene Oxidation," Combustion and Flame, Vol. 71, pp. 295-312, 1988.
9. Dagaut, P., Boetiner, J. C., and Cathonnet, M., "Ethylene Pyrolysis and Oxidation: A Kinetic Modeling Study," Int. J. Chem. Kinet, Vol. 22, pp. 641-664, 1990.
10. Marinov, N. and Malte, .P. "Ethylene Oxidation in a Well-Stirred Reactor", Int. J. Chem. Kinet., Vol. 27, pp. 957-986, 1995.
11. Lindstedt, R.P. and Skevis, G. "Molecular Growth and Oxygenated Species Formation in Laminar Ethylene Flames", Proceedings of the Combustion Institute, 28:1801-1807, 2000.
12. Lindstedt, R.P. and Skevis, G. "Benzene Formation Chemistry in Premixed (1,3)-Butadiene Flames", Proceedings of the Combustion Institute 26, pp. 703-709, 1996.
13. Lindstedt, R.P. and Skevis, G., "Detailed Kinetic Modelling of Premixed Benzene Flames", Combustion and Flame, 99, (1994) pp. 551-561.
14. Lindstedt, R.P. and L.Q. Maurice, "Detailed Kinetic Modelling of Toluene Combustion", Combustion, Science and Technology, 120, (1996) pp. 119-167.
15. Chakir, A., Bellimam, M., Boettner, J. C. and Cathonnet, M., "Kinetic Study of N-Heptane Oxidation," International Journal of Chemical Kinetics, Vol. 24, pp. 385-410, 1992.
16. Lindstedt, R.P. and Maurice, L.Q., "Detailed Kinetic Modelling of n-Heptane Combustion", Combustion, Science and Technology, 107, (1995) pp. 317-353.
17. Dagaut, P., Reuillon, M., and Cathonnet M., "High Pressure Oxidation of Liquid Fuels from Low to High Temperature. 3. n-Decane," Combustion Science and Technology, Vol. 103, pp. 349-359, 1994a.
18. Lindstedt, R.P. and Maurice, L.Q. "A Detailed Chemical Kinetic Model for Aviation Fuels", Journal of Propulsion and Power 16 (2000), pp. 187-195.
19. Lindstedt, R.P., Loloudi, S.A. and Vaos, E.M. "Joint Scalar Probability Density Function Modeling of Pollutant Formation in Piloted Turbulent Jet Diffusion Flames with Comprehensive Chemistry", Proceedings of the Combustion Institute, 28:149-156 (2000).
20. Doute, C., Delfau, J.-L., Akrich, R. and Vovelle, C., "Chemical Structure of Atmospheric Pressure Premixed n-Decane and Kerosene Flames," Combustion Science and Technology, Vol. 106, pp. 327-344, 1995.
21. Dagaut, P., Reuillon, M., Cathonnet, M., and Voisin.., "High Pressure Oxidation of Normal Decane and Kerosen in Dilute Conditions From Low to High Temperature"J. Chim Phys, Vol. 92,pp. 47-76, 1995.
22. Montgomery, C. J., Cannon, S. M., Mawid, M. A., and Sekar, B., "Reduced Chemical Kinetic Mechanisms for JP-8 Combustion," AIAA Paper 2002-0336, 2002.
23. Mawid, M. A., Park, T. W., Sekar, B., and Arana, C., "Importance of Surrogate JP-8/Jet-A Fuel Composition in Detailed Chemical Kinetics Development," AIAA Paper 2004-4207, 40th AIAA/ASME/SAE/ASEE Joint Propulsion Conference and Exhibit, Fort Lauderdale, Florida, July 11-14, 2004.
24. Warnatz, J. "The Structure of Laminar Alkane, Alkene and Acetylene Flames", Eighteenth Symposium International on Combustion/The Combustion Institute, Pittsburgh 1981, p. 369.
25. Axelsson, E. I., Brezinsky, K., Dryer, F. L., Pitz, W. J., and Westbrook, C. K., "Chemical Kinetic Modeling of the Oxidation of Large Alkane Fuels: N-Octane and Iso-Octane," Twenty-First Symposium (International) on Combustion, pp. 783-793, 1986.
26. Schulz, W. D., "Oxidation Products of a Surrogate JP-8 Fuel," Symposium on Structure of Jet Fuels III, San Francisco, CA, pp. 383-392, April 5-10, 1991.
27. Violi, A., Yan, S., Eddings, E. G., Sarofim, A. F., Granata, S., Faravelli, T., and Ranzi, E., "Experimental Formulation and Kinetic Model for JP-8 Surrogate Mixtures," Second Mediterranean Combustion Symposium, Sharm El-Sheik, Egypt, 2002.
28. Gueret, C., Cathonnet, M., Boettner, J.C. and Gaillard, F. "Experimental Study and Modeling of Kerosene Oxidation in a Jet-Stirred Flow Reactor", Proceedings of the Combustion Institute 23, 1990.
29. Dagaut, P., Reuillon, M., Boettner, J.-C., and Cathonnet, M., "Kerosene Combustion at Pressures up to 40 atm: Experimental Study and Detailed Chemical Kinetic Modeling," Proceedings of the Combustion Institute, 25, pp. 919-926, 1994b.
30. Vovelle, C., Delfau, J.L. and Reuillion, M. "Formation of Aromatic Hydrocarbons in Decane and Kerosene Flames at Reduced Pressures" in Soot

Formation in Combustion, Mechanisms and Models, H. Bockhorn Ed., Springer-Verlag, Berlin, 1994.
31. Nehse, M., Warnatz, J., and Chevalier, C., "Kinetic Modeling of the Oxidation of Large Aliphatic Hydrocarbons," Twenty-Sixth Symposium (International) on Combustion, pp. 773-780, 1996.
32. Westbrook, C. K., Warnatz, J., Pitz, W. J., "A Detailed Chemical Kinetic Reaction Mechanism for the Oxidation of Iso-Octane and n-Heptane over an Extended Temperature Range and its Application to Analysis of Engine Knock," Twenty-Second Symposium (International) on Combustion, The Combustion Institute, pp. 893-901, 1988.
33. Chevalier, C., Pitz, W. J., Warnatz, J., Westbrook, C. K., and Melenk, H., "Hydrocarbon Ignition: Automatic Generation of Reaction Mechanisms and Applications to Modeling of Engine Knock," Twenty-Fourth Symposium (International) on Combustion, pp. 93-101, 1992.
34. Warnatz, J., Maas, U., and Dibble, R. W., Combustion, Springer, Heidelberg/Berlin, 1996.
35. Halstead, M. P., Prothero, A., and Quinn, C. P., Proc. R., Soc. London, Ser. A, Vol. 322, pp. 377-403, 1971
36. Westbrook, C. K., Warnatz, J., and Pitz, W. J., Twenty-Second Symposium (International) on Combustion, pp. 553-579, 1992.
37. Pollard, R. T., in Comprehensive Chemical Kinetics, Vol. 17, Gas-Phase Combustion (Bamford, C. H. and Tipper, C. F. H., Eds.), Elsevier, New York, pp. 249-367, 1977.
38. Kaiser, E. W., Westbrook, C. K., and Pitz, W. J., "Acetaldehyde Oxidation in the Negative Temperature Coefficient Regime: Experimental and Modeling Results," International Journal of Chemical Kinetics, Vol. 18, pp. 655-688, 1986.
39. Kojima, S., "Detailed Modeling of n-Butane Autoignition Chemistry," Combustion and Flame, Vol. 99, pp. 87-136, 1994.
40. Warnatz, J. "Chemistry of High Temperature Combustion of Alkans Up To Octane", 20th Symposium (International) on Combustion, pp. 845, 1984.
41. Chevalier, C. and Warnatz, J., "Survey of Reactions in the C/H/O System," in Combustion Chemistry (Gardiner, W. C. Jr., Ed.) Springer Verlag, New York, 1996.
42. Brouwer, L., Muller-Markgraf, W. and Troe, J., "Identification of Primary Reaction Products in the Thermal Decomposition of Aromatic Hydrocarbons," Twentieth Symposium (International) on Combustion, pp. 799-806, 1984.
43. Lindstedt, R.P. and Rizos, K.-A. "The Formation and Oxidation of Aromatics in Cyclopentene and Methyl-Cyclopentadiene Mixtures", Proceedings of the Combustion Institute 29, 2002.
44. Tang, Q., Xu, J. and Pope, S.B. "PDF Calculations of Local Extinction and NO Production in Piloted-Jet Turbulent Methane/Air Flames", Proceedings of the Combustion Institute 28:133-139 (2000).
45. Venkat, C., M.S. Thesis, Chemical Engineering Department, Princeton University, 1981.
46. Emdee, J.L, Brezinsky, K. And Glassman, I., "A Kinetic Model for the Oxidation of Toluene Near 1200 K," Journal of Physical Chemistry, v. 96, pp. 2151, 1992.
47. Dagaut, P., Ristori, A., El Bakali, A. and Cathonnet, M. "Experimental and Kinetic Modelling of the Oxidation of n-Propylbenzene," Fuel 81:173-184, 2002.
48. Kee, R. J., Rupley, F. M., Meeks, E., and Miller, J. A., "CHEMKIN-III: A Fortran Chemical Kinetics Package for the Analysis of Gas-phase Chemical and Plasma Kinetics," SANDIA Report SAND96-8216, 1996.
49. Benson, S. W., Thermochemical Kinetic, John Wiley and Sons, New York, pp. 164-169, 1968.
50. Burcat, A., Thermochemical Data for Combustion Calculations, Combustion Chemistry, Gardiner, W. C., Jr., Ed., Springer-Verlag, New York, Chap. 8, pp.455, 1984.
51. Freeman, G. and Lefebrve, A. H., "Spontaneous Ignition Characteristics of Gaseous Hydrocarbon-Air Mixtures," Combustion and Flame, Vol. 58, pp. 153-162, 1984.
52. Mullins, B. P., "Autoignition of Hydrocarbons," AGARDograph, No. 4, 1955.
53. Larson, R. S., "PLUG: A Fortran Program for the Analysis of Plug Flow Reactors with Gas-Phase and Surface Chemistry," SANDIA Report SAND96-8211, 1996.
54. Glarborg, P., Kee, R. J., Grcar, J. F., and Miller, J. A., "PSR: A Fortran Program for Modeling Well-Stirred Reactors," SANDIA Report SAND86-8209, 1986.

Table I

JP-8 Fuel Components	JP-8 Surrogate-1 Volume %	JP-8 Surrogate-2 Volume %	JP-8 Surrogate-3 Volume %
n-decane (n-C10H22)	16.2	0	25.0
n-dodecane (n-C12H26)	21.0	30.0	25.0
n-tetradecane (n-C14H30)	15.6	20.0	20.0
n-hexadecane (n-C16H34)	10.2	0	0
i-octane (i-C8H18)	5.7	10.0	5.0
cyclooctane (c-C8H16)	4.7	0	0
methylcyclohexane,MCH (C7H14)	5.1	20.0	5.0
1-methylnaphthalene (C11H10)	3.9	0	0
tetralin (C10H12)	4.1	5.0	0
1,2,4,5-tetramethylbenzene (C9H12)	4.4	0	0
butylbenzene (C10H14)	4.6	0	0
m-xylene (C8H10)	4.5	15.0	0
toluene (C7H8)	0	0	20.0

Table II High Temperature C12H26 Submechanism (reactions given are only for primary C-H bonds)

Reaction	A cm-gm-sec	α	E cal/mole
Dodecane(NC12H26)			
NC12H26 = C6H12 + NC6H14	3.20E+16	0.00	80968.76
NC12H26 + O2 = C12H25 + HO2	1.00E+13	0.00	47530.33
NC12H26 + HO2 = C12H25 + H2O2	1.60E+12	0.00	17005.83
NC12H26 + H = C12H25 + H2	4.50E+06	2.00	4991.88
NC12H26 + OH = C12H25 + H2O	6.50E+08	1.25	702.21
NC12H26 + O = C12H25 + OH	1.30E+13	0.00	5206.84
NC12H26 + CH3 = C12H25 + CH4	2.00E+11	0.00	9506.07
C12H25 = C10H21 + C2H4	2.50E+13	0.00	28661.51
C10H21 = C8H17 + C2H4	2.50E+13	0.00	28800.00
C10H21 + HO2 = C9H19 + CH2O + OH	2.00E+13	0.00	0.00
C10H21 + O = C9H19 + CH2O	5.00E+13	0.00	0.00
C9H19 = C7H15 + C2H4	2.52E+13	0.00	28800.00
C7H15 = C7H14 + H	4.26E+13	0.00	38600.00
C7H14 = C2H3 + C5H11	1.00E+19	-1.00	96770.00
C7H14 + O2 = C7H13 + HO2	1.40E+13	0.00	31900.00
C7H14 + HO2 = C7H13 + H2O2	1.00E+11	0.00	17060.00
C7H14 + OH = C7H13 + H2O	6.30E+06	2.00	-543.00
C7H14 + CH3 = C7H13 + CH4	2.00E+11	0.00	6800.00
C7H13 = C6H12 + H	1.30E+13	0.00	39000.00

Table III Low Temperature Mechanism

Reaction	A cm-gm-sec	α	E cal/mole
Dodecane			
NC12H26 = C6H12 + NC6H14	3.20E+16	0.00	80968.76
C12H25 + O2 → C12H25O2	2.00E+12	0.00	0.00
C12H25O2 → C12H25 + O2	4.00E+15	0.00	117.00
C12H25 + O2 → C12H24 + HO2	1.00E+12	0.00	8.40
C12H24 + HO2 → C12H25 + O2	1.70E+12	0.00	57.60
C12H25O2 → C12H24O2H	1.00E+11	0.00	71.20
C12H24O2H → C12H25O2	1.00E+11	0.00	52.30
C12H24O2H → C12H24O + OH	3.00E+11	0.00	58.60
C12H24O2H → C12H24 + HO2	3.00E+11	0.00	83.80
C12H24OOH + O2 ↔ O2C12H24O2H	2.00E+12	0.00	0.00
O2C12H24O2H → HO2C12H24O2H	1.00E+11	0.00	71.20
HO2C12H24O2H → O2C12H24O2H	1.00E+11	0.00	52.30
HO2C12H24O2H → HO2C12H24O + OH	1.00E+09	0.00	31.40
HO2C12H24O2H → OC12H24O + OH	8.40E+14	0.00	180.00
HO2C12H24O → C5H11CHO + C5H12CO2H	2.50E+13	0.00	120.00
OC12H24O → C5H11CHO + C5H11CHO	2.50E+13	0.00	120.00
C5H12CO2H → C5H12 + CO2 + H	1.58E+13	0.00	72.00
C5H11CHO + OH → C5H11CO + H2O	1.75E+13	0.00	0.00
C5H11CHO + O2 → C5H11CO + HO2	2.00E+13	0.50	175.00
C5H11CHO + HO2 → C5H11CO + H2O2	1.00E+12	0.00	42.00
C5H11CHO + CH3O2 → C5H11CO + CH2O2H	1.00E+12	0.00	42.00
C5H11CO + O2 → C5H10COO2H	2.00E+14	0.00	150.00
C5H10COO2H → C5H10 + CO2 + OH	1.00E+12	0.00	10.00
C5H11CO → C5H11 + CO	1.58E+13	0.00	72.00

Table IV

Reaction	A cm-gm-sec	α	E cal/mole
Benzen			
C6H6 = C4H4 + C2H2	9.000E+15	0.0	107430.0
C6H6 + O2 = C6H5 + HO2	6.300E+13	0.0	60057.0
C6H6 + HO2 = C6H5 + H2O2	1.520E+11	0.0	17000.0
C6H6 + HO2 => C6H5O + OH + H	2.520E+12	0.0	14340.0
C6H6 + OH = C6H5 + H2O	1.061E+13	0.0	3683.0
C6H6 + H = C6H5 + H2	2.500E+14	0.0	16000.0
C6H6 + CH3 = C6H5 + CH4	2.000E+12	0.0	15057.0
C6H6 + C2H5 = C6H5 + C2H6	6.310E+11	0.0	14866.0
C6H6 + C5H5 = C6H5 + C5H6C	6.310E+11	0.0	14866.0
C6H5 = C2H2 + C4H3	6.310E+14	0.0	83000.0
C6H5 = C2H3 + C4H2	1.200E+15	0.0	82000.0
C6H5 + O2 = C6H5O + O	6.270E+12	0.0	7470.0
C6H5 + C2H2 = C8H6 + H	3.200E+11	0.0	1391.0
C6H5 + C2H4 = C8H8 + H	3.160E+11	0.0	1940.0
C6H5 + C4H2 = C8H6 + C2H	2.000E+13	0.0	0.0
C6H5 + C4H4 = C8H6 + C2H3	3.200E+11	0.0	1350.0
C6H5O => C5H5 + CO	7.530E+11	0.0	43900.0
C6H5O + H = C6H5OH	8.360E+13	0.0	0.0
C6H5OH + OH = C6H5O + H2O	6.000E+12	0.0	0.0

C6H5OH	+	H	=	C6H6	+	OH			2.210E+13	0.0	7910.0
C6H5OH	+	H	=	C6H5O	+	H2			1.150E+14	0.0	12400.0
C6H5OH	+	O	=	C6H5O	+	OH			1.280E+13	0.0	2891.0
C6H5OH	+	C2H3	=	C6H5O	+	C2H4			6.000E+12	0.0	0.0
C6H5OH	+	C4H5	=	C6H5O	+	C4H6			6.000E+12	0.0	0.0

Toluene

C7H8			=	C6H5	+	CH3			1.400E+16	0.0	99800.0
C7H8			=	C7H7	+	H			1.150E+16	0.0	91140.0
C7H8	+	O2	=	C7H7	+	HO2			3.000E+14	0.0	41400.0
C7H8	+	HO2	=	C7H7	+	H2O2			1.470E+11	0.0	19377.0
C7H8	+	OH	=	C7H7	+	H2O			1.200E+13	0.0	2367.0
C7H8	+	O	=	C7H7	+	OH			6.300E+11	0.0	0.0
C7H8	+	H	=	C7H7	+	H2			2.260E+02	3.478	2640.0
C7H8	+	CH3	=	C7H7	+	CH4			8.880E+10	0.0	8754.0
C7H8	+	C2H5	=	C7H7	+	C2H6			1.008E+11	0.0	9514.0
C7H8	+	C3H5	=	C7H7	+	C3H6			3.980E+12	0.0	7472.0
C7H8	+	C6H5	=	C7H7	+	C6H6			2.100E+12	0.0	4400.0
C7H7			=	C4H4	+	C3H3			2.000E+14	0.0	70000.0
C7H7			=	C5H5	+	C2H2			6.030E+13	0.0	83600.0
C7H7	+	O2	=	C6H5O	+	CH2O			3.000E+10	0.0	2870.0
C7H7	+	HO2	=>	C7H6O	+	OH	+	H	1.700E+13	0.0	0.0
C7H7	+	HO2	=>	C6H5	+	CH2O	+	OH	2.000E+13	0.0	0.0
C7H7	+	OH	=	C7H7OH					2.000E+13	0.0	0.0
C7H7	+	O	=	C7H6O	+	H			1.580E+13	0.0	0.0
C7H7	+	O	=	C6H5	+	CH2O			8.000E+13	0.0	0.0
C7H7	+	C2H2	=	C7H8	+	C2H			1.000E+12	0.0	0.0
C7H7	+	C3H3	=	C7H8	+	C3H2			1.000E+12	0.0	0.0
C7H7	+	C6H5OH	=	C7H8	+	C6H5O			1.050E+11	0.0	9500.0
C7H7	+	C7H6O	=	C7H5O	+	C7H8			2.770E+03	2.81	5773.0
C7H7OH	+	O2	=>	C7H6O	+	HO2	+	H	2.000E+14	0.0	41400.0
C7H7OH	+	OH	=>	C7H6O	+	H2O	+	H	8.430E+12	0.0	2583.0
C7H7OH	+	H	=	C6H6	+	CH2OH			1.200E+13	0.0	5148.0
C7H7OH	+	C7H7	=>	C7H6O	+	C7H8	+	H	2.110E+11	0.0	9500.0
C7H7OH	+	C6H5	=>	C7H6O	+	C6H6	+	H	1.400E+12	0.0	4400.0
C7H6O			=	C7H5O	+	H			3.980E+15	0.0	83701.0
C7H6O	+	O2	=	C7H5O	+	HO2			1.020E+13	0.0	39000.0
C7H6O	+	HO2	=	C7H5O	+	H2O2			2.000E+12	0.0	11665.0
C7H6O	+	OH	=	C7H5O	+	H2O			1.710E+09	1.18	-447.0
C7H6O	+	OH	=	C6H5OH	+	HCO			1.200E+13	0.0	5123.0
C7H6O	+	O	=	C7H5O	+	OH			9.040E+12	0.0	3080.0
C7H6O	+	H	=	C7H5O	+	H2			5.000E+13	0.0	4928.0
C7H6O	+	H	=	C6H6	+	HCO			1.200E+13	0.0	5148.0
C7H6O	+	CH3	=	C7H5O	+	CH4			2.770E+03	2.81	5773.0
C7H6O	+	C6H5	=	C7H5O	+	C6H6			7.010E+11	0.0	4400.0
C7H5O			=	C6H5	+	CO			3.980E+14	0.0	29401.0
C7H5O	+	O2	=	C6H5O	+	CO2			3.000E+10	0.0	2870.0
C7H5O	+	HO2	=>	C6H5	+	CO2	+	OH	2.000E+13	0.0	0.0

m-xylene

C8H10			=	C6H6	+	C2H4			1.00E+10	0.00	80000.0
C8H10	+	O2	=	C8H9	+	HO2			1.00E+11	0.00	25050.0
C8H10	+	HO2	=	C8H9	+	H2O2			1.636E+11	0.00	12583.0
C8H10	+	OH	=	C8H9	+	H2O			5.60E+12	0.00	861.0
C8H10	+	H	=	C8H9	+	H2			1.00E+14	0.00	3900.0
C8H10	+	CH3	=	C8H9	+	CH4			2.50E+11	0.00	8300.0
C8H10	+	C2H5	=	C8H9	+	C2H6			1.00E+11	0.00	8300.0
C8H10	+	C2H3	=	C8H9	+	C2H4			6.30E+12	0.00	13000.0
C8H9			=	C6H5	+	C2H4			3.16E+14	0.00	37700.0

Table V

JP-8 Fuel Components	JP-8 Surrogate-1 Mole Fraction	JP-8 Surrogate-3 Mole Fraction
n-decane (n-C10H22)	9.98070E-04	1.66765E-03
n-dodecane (n-C12H26)	1.11158E-03	1.66765E-03
n-tetradecane (n-C14H30)	7.15788E-04	1.33412E-03
n-hexadecane (n-C16H34)	4.18071E-04	0.0
i-octane (i-C8H18)	4.14403E-04	3.33530E-04
cyclooctane (c-C8H16)	4.21803E-04	0.0
methylcyclohexane,MCH (C7H14)	4.82061E-04	3.33530E-04
1-methylnaphthalene (C11H10)	3.32690E-04	0.0
tetralin (C10H12)	3.57894E-04	0.0
1,2,4,5-tetramethylbenzene (C9H12)	3.93683E-04	0.0
butylbenzene (C10H14)	3.52552E-04	0.0
m-xylene (C8H10)	4.45679E-04	0.0
toluene (C7H8)	0.0	1.33412E-03
oxygen (O2)	2.08150E-01	2.10124E-01
nitrogen (N2)	7.85406E-01	7.83205E-01